water

MDPI

Article

Comprehensive Effects of Atmosphere and Soil Drying on Stomatal Behavior of Different Plant Types

Zhi Xu [1], Ye Tian [2,*], Zhiwu Liu [1] and Xinran Xia [2]

[1] Institute of Science and Technology, China Three Gorges Corporation, Beijing 100038, China
[2] Hydrology and Water Resources Department, Nanjing University of Information Science & Technology, Nanjing 210044, China
* Correspondence: tianye@nuist.edu.cn

Abstract: The soil water supply and atmospheric humidity conditions are crucial in controlling plants' stomatal behavior and water use efficiency. When there is water stress caused by an increase in saturated water vapor pressure (VPD) and a decrease in soil water content (SWC), plants tend to close stomata to reduce water loss. This affects the gross primary productivity (GPP) and evapotranspiration (ET), subsequently leading to changes in water use efficiency (WUE) and carbon use efficiency (CUE) in plants. However, land–atmosphere interactions mean that water vapor in the atmosphere and soil moisture content causing water stress for plants are closely related. This study aims to compare and estimate the effects of VPD and SWC on the carbon cycle and water cycle for different plant functional types. Based on the fluxnet2015 dataset from around the world, the WUE and CUE of five plant functional types (PFTs) were estimated under varying levels of VPD and SWC. The results showed that high VPD and low SWC limit the stomatal conductance (Gs) and gross primary productivity (GPP) of plants. However, certain types of vegetation (crops, broad-leaved forests) could partially offset the negative effects of high VPD with higher SWC. Notably, higher SWC could even alleviate limitations and partially promote the increase in GPP and net primary production (NPP) with increasing VPD. WUE and CUE were directly affected by Gs and productivity. In general, the increase in VPD in the five PFTs was the dominant factor in changing WUE and CUE. The impact of SWC limitations on CUE was minimal, with an overall impact of only $-0.05\mu mol/\mu mol$ on the four PFTs. However, the CUE of savanna plants changed differently from the other four PFTs. The rise in VPD dominated the changes in CUE, and there was an upward trend as SWC declined, indicating that the increase in VPD and decrease in SWC promote the increase in the CUE of savanna plants to some extent.

Keywords: stomatal behavior; water use efficiency; carbon use efficiency; water vapor pressure; soil water content

check for updates

Citation: Xu, Z.; Tian, Y.; Liu, Z.; Xia, X. Comprehensive Effects of Atmosphere and Soil Drying on Stomatal Behavior of Different Plant Types. *Water* **2023**, *15*, 1675. https://doi.org/10.3390/w15091675

Academic Editor: Guido D'Urso

Received: 20 March 2023
Revised: 17 April 2023
Accepted: 21 April 2023
Published: 25 April 2023

1. Introduction

Vapor pressure deficit (VPD) and soil water content (SWC) are two important environmental factors that influence vegetation photosynthetic efficiency, gross primary productivity (GPP), and net primary productivity (NPP) [1,2]. Photosynthesis is the primary pathway for vegetation to obtain energy and organic matter, absorbing carbon dioxide through the stomata while releasing water vapor during the transpiration process. GPP refers to the total amount of solar energy fixed by plants through photosynthesis, including the energy used in biochemical reactions and the energy lost during photosynthesis. NPP, on the other hand, is the remaining energy after subtracting the energy used for plant growth and reproduction from GPP. Thus, GPP represents the total energy obtained by plants through photosynthesis, while NPP represents the net energy used for growth and reproduction.

Sufficient soil moisture provides the necessary water supply for vegetation, allowing for optimal water uptake through roots for photosynthesis and biomass accumulation.

However, a decrease in SWC leads to a decrease in the available water taken in by plant roots [3]. Insufficient soil moisture can have negative impacts on vegetation productivity, limiting photosynthesis and biomass accumulation, leading to decreased GPP and NPP [4,5], while an increase in VPD will induce plants to close stomata to minimize leaf-scale water loss and further inhibit plant photosynthesis in the ecosystem [6,7], and lower photosynthetic efficiency usually indicates reduced utilization of light energy for photosynthesis and lower production of organic matter. This is because plants need to adjust stomatal conductance to maximize carbon gains and reduce water loss as much as possible under the condition of high VPD. Evidently, this process will affect the carbon cycle and water cycle of the ecosystem [8,9].

Vegetation water use efficiency (WUE) and carbon use efficiency (CUE) are important parameters that describe how plants utilize water and carbon during photosynthesis. Vegetation water use efficiency refers to the amount of water required by plants to produce a unit of biomass during photosynthesis, while carbon use efficiency refers to the amount of carbon fixed through photosynthesis that is allocated to plant growth and reproduction [10,11]. There is a complex relationship between GPP, NPP, photosynthesis, vegetation water use efficiency, and carbon use efficiency. Higher GPP and NPP are generally associated with higher photosynthesis rates, as more solar energy is captured and converted into organic matter. This may result in higher vegetation water use efficiency, as plants can produce more biomass with less water. Similarly, higher carbon use efficiency may be observed, as more carbon is allocated to plant growth and reproduction [12].

In recent years, many studies have emphasized the importance of VPD and SWC on plant stomatal conductance (Gs) and evaluated their sensitivity and contributions. Novick et al. [13] found that in many biomes, VPD had greater restrictions on stomatal conductance (Gs) and evapotranspiration (ET) than SWC. In the future, the impact of atmospheric demand on vegetation function will become more and more important, accounting for more than 70% of the surface conductance limit in the growing season of temperate forests. Sulman et al. [14] showed that ecosystem-scale transpiration and photosynthesis were significantly correlated with VPD and SWC, and VPD was the main contributor to the interannual changes in photosynthesis and transpiration in temperate forest sites. The analysis of crops also showed that the Gs difference was mainly due to the change in VPD, which was almost unrelated to the changes in environmental conditions (rainfall and temperature gradient), crop types (corn and soybean), and management practices (irrigated or not) [15]. In addition, plant water use efficiency (WUE) is also affected by VPD and SWC. There is a significant negative correlation between WUE and SWC in the ecosystem, and the negative correlation is more obvious at higher VPD [16,17]. One study points out that the WUE of the ecosystem will increase by 10–35% at the end of this century with the rise in VPD under Representative Concentration Pathway 8.5 (RCP8.5) [18], which is supported by both observation and model simulation [19–21]. In contrast, the research on how plant carbon use efficiency (CUE) is affected by VPD and SWC is not sufficient, especially the systematic and comprehensive discussion on CUE and its influencing factors [22].

However, WUE and CUE efficiency can be influenced by various factors, such as environmental conditions, plant species, and physiological processes [23]. Under drought conditions, plants may reduce transpiration to minimize water loss, which can lead to lower GPP and NPP, as plants are limited by water availability [24–26]. This may also result in lower vegetation water use efficiency, as plants need to use more water to produce the same amount of biomass. There is ongoing debate about whether VPD or SWC has more influence on plant water stress, given that they interact with each other and other climatic variables in land–atmosphere interactions [27–29]. For instance, precipitation directly affects atmospheric temperature and SWC, and in return, SWC feeds back into the atmosphere relative humidity, which could determine the change in VPD with the concurrent effect of the atmospheric temperature [8,9,30,31]. Furthermore, with future global warming, the compound adverse effects of increasing VPD and decreasing SWC on plants and ecosystems may make the problem more complex and critical [15,32]. Therefore, research is needed to better understand the complex interactions between GPP, NPP, photosynthesis, vegetation water use efficiency, and carbon use efficiency. This knowledge can provide insights into plant productivity and resource utilization in ecosystems, and contribute to better management and conservation strategies for natural resources.

In summary, to clarify the relationship between VPD and SWC and plant stomatal behavior and carbon and water use efficiency, and systematically evaluate the response of different ecosystems to water stress, we used the hourly observation data of 36 flux towers covering five plant functional types (PFTs) from around the world, namely crops, deciduous broad-leaved forest, evergreen coniferous forest, grassland, and savanna. This paper delves into the impact of VPD and SWC on the carbon and water cycles of ecosystems, specifically through their influence on plant stomatal behavior. Additionally, this paper aims to elucidate how different PFTs are differentially affected by VPD and SWC, and to identify the conditions under which certain PFTs are most susceptible. Through a detailed investigation of VPD and SWC's impact on plant stomatal behavior, CUE, and WUE in varying PFTs, this paper seeks to enhance our understanding of the relationship between hydrological and climatic factors and ecosystem functioning. Ultimately, the findings of this study can serve as an important reference for future research on the role of plants in ecosystem carbon and water cycling.

2. Materials and Methods

2.1. Data

The FLUXNET2015 dataset (http://fluxnet.fluxdata.org/data/Fluxnet2015dataset/, accessed on 16 June 2020) is a global dataset of eddy covariance flux measurements, which are used to estimate the exchange of carbon dioxide, water vapor, and energy between the terrestrial ecosystem and the atmosphere. Hourly and half-hourly eddy covariance measure-related fluxes and meteorological data were selected for the study. The FLUXNET2015 dataset categorizes plant functional types (PFTs) into broad groups based on their growth form and ecological characteristics, such as forests, grasslands, croplands, wetlands etc.

The selected data from all the stations of fluxnet2015 Tier1 meet the requirement that they have continuously available data for at least three years, and the meteorological indicators include temperature (ta), precipitation (P), vapor pressure difference (VPD), soil water content (SWC), wind speed (WS), friction velocity (USTAR), soil heat flux (G), latent heat flux (LE), sensible heat flux (H), net radiation (Rn), gross primary productivity (GPP), and ecosystem respiration (RECO) [33,34]. The location and information of the stations are shown in Figure 1 and Table S1. FLUXNET data are observed and quality-controlled according to unified standards, including friction velocity filtering and missing measured value filling. Finally, 36 sites from around the world were selected, which cover five plant functional types (PFTs), namely crops (CRO, station 9), deciduous broad-leaved forest (DBF, station 5), evergreen coniferous forest (ENF, station 6), grassland (GRA, station 10), and savanna (SAV, station 6).

CRO typically refers to agricultural lands that are managed for crop production, such as row crops including corn, wheat, soybeans, and other cultivated lands. These areas are characterized by annual or seasonal vegetation that is typically managed through planting, harvesting, and other agricultural practices. DBF represents forests dominated by deciduous broad-leaved tree species, which are known for their seasonal leaf turnover. ENF represents forests dominated by evergreen coniferous tree species, such as pine, spruce, and fir. Evergreen coniferous forests are characterized by trees that retain their needles throughout the year, allowing them to photosynthesize and maintain their green color. GRA typically refers to ecosystems dominated by grasses as the main vegetation type, with little or no tree cover. They have important ecological roles, such as supporting grazing animals, carbon storage, and fire regimes. SAV typically refers to ecosystems that are characterized by a mix of grasses and trees, with an open canopy structure. Savannas play important roles in biodiversity conservation, carbon storage, and the livelihoods of local communities.

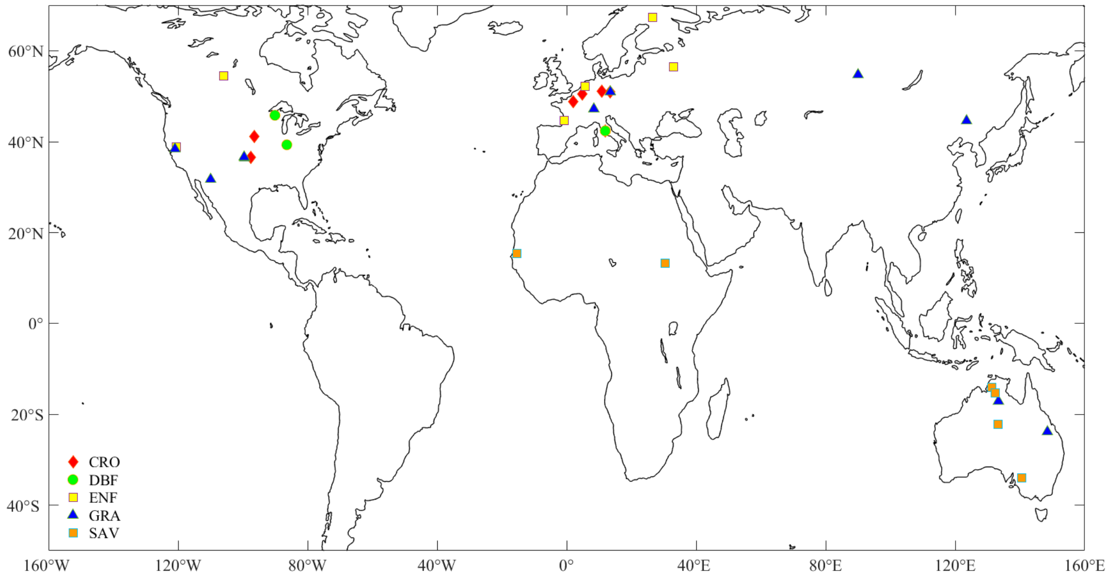

Figure 1. Global distribution of 36 flux stations (5 PFTs are included: CRO, DBF, ENF, GRA, and SAV).

To ensure there are enough stations for each type, a number of stations with limited observation time spans did not pass the quality check. Thus, plant functional types including evergreen broad-leaved forest (EBF), mixed forest (MF), and shrub (CSH) are not considered in this study, while wetland (WET) is also excluded due to the lack of measurement of soil heat flux.

2.2. Methods

2.2.1. Estimation of the Stomatal Conductance

Based on the Penman–Monteith formula, vegetation stomatal conductance can be estimated using flux measurement [35]. The formula is as follows:

$$\mathrm{Gs} = \frac{\gamma LE g_a}{\Delta(R_n - G) - LE(\gamma + \Delta) + \rho C_p VPD g_a} \tag{1}$$

In the equation, Gs is the stomatal conductance (m s^{-1}), γ (kPa °C^{-1}) is the hygrometer constant, *LE* (W m^{-2}) is the latent heat flux, Δ (kPa °C^{-1}) is the slope of saturated vapor pressure and temperature, R_n (W m^{-2}) is the net radiation flux, G (W m^{-2}) is the soil heat flux, ρ (kg m^{-3}) is the air density, C_p (J kg^{-1} °C^{-1}) is the specific heat capacity of air, *VPD* (kPa) is the saturated water vapor pressure difference, and $\mathrm{g_a}$ (m s^{-1}) is the aerodynamic conductivity. In this paper, the relationship between canopy height and wind speed proposed by Campbell and Norman is used to estimate g_a [36]:

$$g_a = \frac{U\mathrm{K}^2}{\left[\ln\left(\frac{z_m - z_d}{z_0}\right)\right]^2} \tag{2}$$

where U (m s^{-1}) represents the wind speed, K is the von Karman constant (K = 0.4), z_m (m) is the measured height, z_d (m) is the zero plane displacement, and z_0 (m) is the momentum roughness length. z_d and z_0 are taken as 0.67 h and 0.1 h, respectively, while h is the canopy height.

2.2.2. Calculation of Water Use Efficiency and Carbon Use Efficiency

WUE refers to [18], and water use efficiency at the ecosystem scale is defined as the specific stomatal conductance (*Gs*) of gross primary productivity (*GPP*):

$$WUE = \frac{GPP}{Gs} \tag{3}$$

WUE (μmol/mol) is the water use efficiency. *GPP* is obtained through the nighttime method (GPP_NT_VUT) in the flux data [37], and the unit is μmol m^{-2} s^{-1}. *Gs* is stomatal conductance, and the unit needs to be converted into (mol m^{-2} s^{-1}).

CUE (μmol/μmol) [38] is defined as the ratio of plant net primary productivity to total primary productivity:

$$CUE = \frac{NPP}{GPP} = \frac{GPP - RECO}{GPP} \tag{4}$$

where *NPP* (μmol m^{-2} s^{-1}) is the net primary productivity of plants, *GPP* (μmol m^{-2} s^{-1}) is the total primary productivity of plants, *RECO* (μmol m^{-2} s^{-1}) is ecosystem respiration, including the autotrophic respiration and heterotrophic respiration of plants, in which *GPP* and *RECO* are directly measured by the flux tower. In this paper, *GPP*–*RECO* is used to approximate the *NPP* of plant net primary productivity [27].

2.2.3. Separating the Relative Contribution of SWC and VPD to WUE and CUE

Liu et al. [1] used SIF and reanalysis climate data for a global analysis. They estimated the difference between the SIF of the highest VPD bin and the lowest VPD bin in each SWC bin to derive ΔSIF (VPD | SWC), which means VPD limitation of SIF without SWC–VPD coupling. Similarly, the difference between the SIF of the highest SWC bin and the lowest SWC bin in each VPD bin is called ΔSIF (SWC | VPD). This method can quantify the SWC and VPD limitation of SIF without SWC–VPD coupling. In this paper, we refer to this method and apply it to WUE and CUE. We calculate the ΔWUE (VPD | SWC), ΔWUE (SWC | VPD), Δ CUE (VPD | SWC), and ΔCUE (SWC | VPD) of each site. The specific calculation formula is as follows:

$$\Delta Var(VPD|SWC) = \frac{1}{n}\sum_{i=1}^{n} Var_{i,max} - Var_{i,min} \tag{5}$$

where *Var* is WUE or CUE, *n* is the number of *SWC* bins, and *i* is the bin number of a specific SWC bin. *i*, *max* and *i*, *min* are the maximum and minimum VPD bin numbers in *SWC* bin *i*, respectively. This formula can calculate the limit of VPD rise in WUE and CUE without SWC–VPD coupling (termed Δ*Var (VPD | SWC)*). Similarly, the limit of SWC reduction in WUE and CUE without SWC–VPD coupling (called Δ*Var (SWC | VPD)*) is calculated as follows:

$$\Delta Var(SWC|VPD) = \frac{1}{m}\sum_{j}^{m} Var_{j,min} - Var_{j,max} \tag{6}$$

where *M* is the number of *SWC* bins and *j* is the bin number of a specific VPD bin. *j*,*min* and *j*,*max* are the minimum and maximum *SWC* bin numbers in *VPD* bin *j*, respectively. The response of plant photosynthesis to *SWC* and *VPD* can be nonlinear [39], which can be overcome by using this method.

Many previous studies have shown that the correlation between VPD and SWC decreases with a decreasing time scale [14,32], and the correlation coefficient between the two is very low at the hourly scale, indicating negligible mutual influence. Therefore, in order to decouple the effects of VPD and SWC as much as possible, hourly data were used in the analysis presented in this paper. SWC is divided into six percentile ranges: 0–15%, 15–30%, 30–50%, 50–70%, 70–90%, and 90–100%. The site meteorological and flux data are classified accordingly into these six ranges. The data were further classified using VPD, with a VPD range of 0.2 kPa selected to ensure sufficient data in each VPD bin. To reduce the impact of outliers, only the mean values of data with more than 10 samples in each bin were selected to represent the quantity of different indicators in each VPD and SWC range.

3. Results

3.1. Meteorology Characteristics of Sites

Figure 2 shows the ranges of the four main climate variables, VPD, SWC, shortwave radiation (SWin), and 2 m air temperature (Ta), that affect the plant stomatal behavior. It can be seen that there are significant differences in VPD and SWC among the five vegetation types. The SWC of the ENF, GRA, and SAV sites is significantly lower than that of CRO and DBF sites, with most of the SWC of SAV sites being below 10%. The VPD of GRA and SAV sites is commonly 5–10 hPa higher than that of ENF, COR, and DBF sites. It is evident that the water demand from the atmosphere and soil water deficit in GRA and SAV sites lead to significantly greater water stress than in CRO, DBF, and ENF sites.

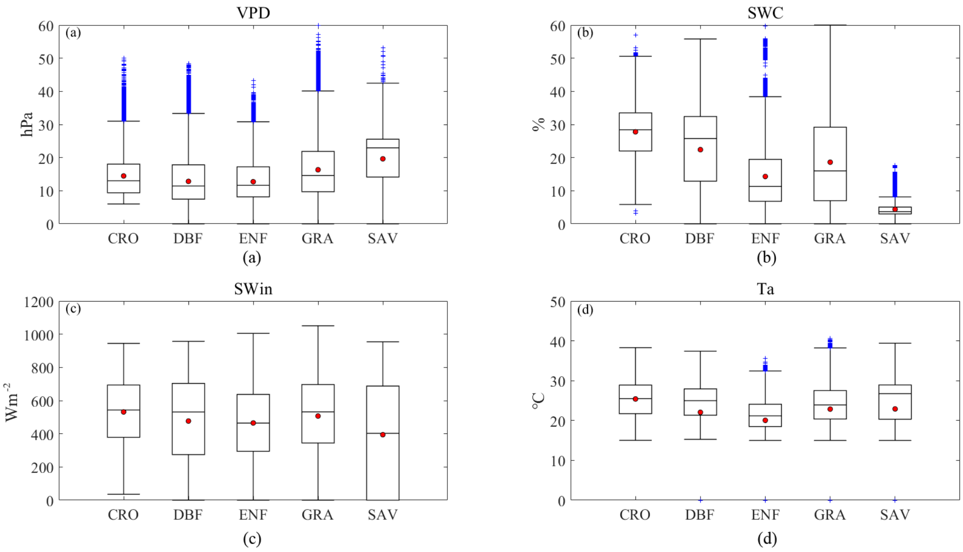

Figure 2. Ranges of four variables (**a**) VPD, (**b**) SWC, (**c**) SWin, and (**d**) Ta for five PFT (CRO, DBF, ENF, GRA, and SAV) sites. The upper, middle, and lower horizontal lines represent the 75th percentile, median, and 25th percentile, respectively. The red dot represents the mean value, and the blue '+' sign represents an abnormal value.

3.2. Effect of Decoupling VPD and SWC on Vegetation Stomatal Behavior

Figure 3 illustrates the distribution of Gs, GPP, and NPP across five vegetation types, where Gsref, GPPref, and NPPref represent the plant reference stomatal conductance, primary productivity, and net primary productivity (defined as the mean of VPD between 0.9 and 1.1 kPa), respectively.

For the CRO and DBF sites, when the SWC percentile is in the 90–100% range, Gs shows a very slow increasing trend with increasing VPD compared to other SWC ranges, which may imply that extremely high SWC weakens the limiting effect of increasing VPD on Gs, and may even promote an increase in Gs in the opposite direction. Analyzing the impact of SWC on Gs across the five vegetation types reveals that there is a large difference in Gs among different SWC percentile ranges, and the difference in Gs/Gsref is even greater than 1 when VPD is around 1 kPa.

Overall, except for the SAV sites, the Gs of the other four vegetation types decrease with decreasing SWC, with the CRO and GRA showing the most significant SWC limitation, while the relationship between SWC and Gs in the SAV sites differs from that of other vegetation types, as Gs is almost greater in all VPD ranges when SWC is low (0–30%) than when it is high (30–70%). This phenomenon may be due to the overall low and stable SWC at the SAV sites, where slightly lower SWC may be more favorable for plant stomatal opening.

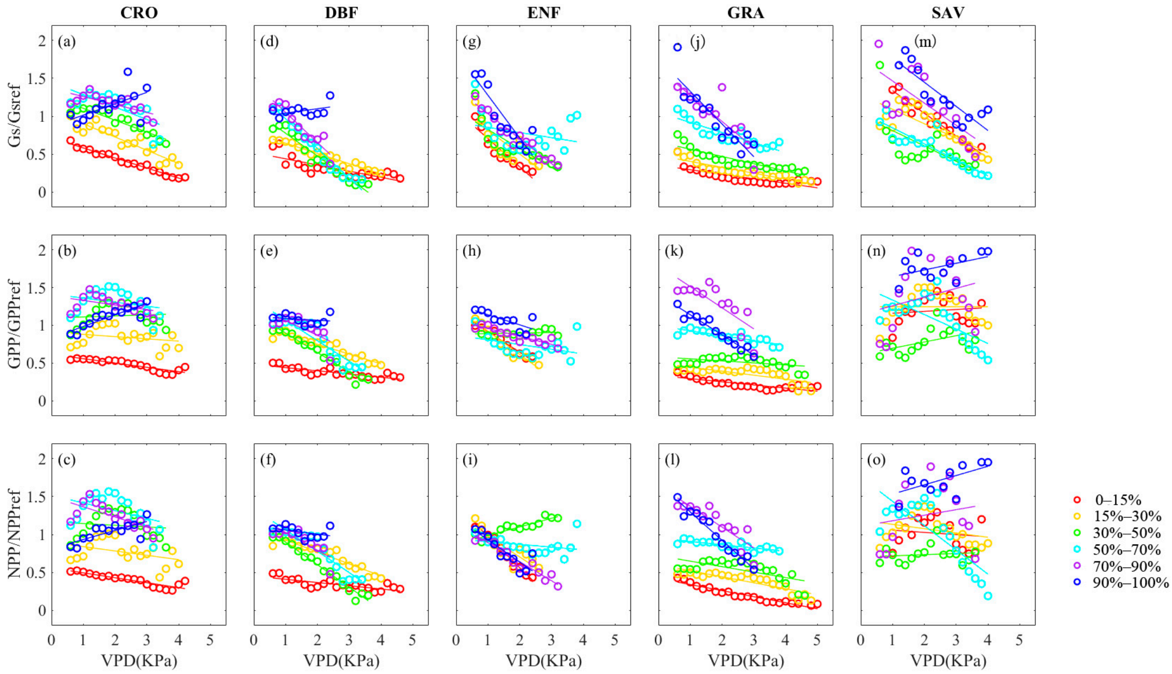

Figure 3. The influence of Gs, GPP, and NPP on five PFTs ((**a**–**c**) CRO, (**d**–**f**) DBF, (**g**–**i**) ENF, (**j**–**l**) GRA, (**m**–**o**) SAV) when VPD and SWC are decoupled. The six colors represent different percentile ranges of soil water content (0–15%, 15–30%, 30–50%, 50–70%, 70–90%, and 90–100%). The interval of each point on VPD is 0.2 kpa.

In contrast to Gs, the GPP of the five vegetation types reflects different characteristics, with DBF, ENF, and GRA showing an overall decrease in GPP with increasing VPD, which is also affected by SWC. The GPP with a high SWC range (70–100%) in the DBF and the GRA sites is significantly larger than the low SWC range (0–15%) at various VPD values, and the difference between them gradually decreases with increasing VPD, while the ENF is less affected by SWC, with similar GPP values across all VPD ranges. The GPP variation in the CRO sites reveals that GPP does not show any obvious limitation effects in various VPD ranges, but instead increases with increasing VPD at higher SWC (90–100%), which is possibly affected by human activities, indicating that the effect of VPD limitation on GPP in CRO with different SWC conditions is not significant. The GPP variation in SAV is clearly different from the previous four vegetation types, with a general trend of increasing first and then decreasing, where GPP increases with increasing VPD when VPD is less than 2 kPa and starts to decrease when VPD is greater than 2 kPa, but is not limited by VPD in the high SWC range (90–100%). The GPP in SAV sites is also limited by SWC, where similar to Gs distribution, the GPP value in the low SWC range (0–30%) is greater than that in the high SWC range (30–50%).

The comparison of NPP distribution shows that the basic characteristics are consistent with GPP distribution, indicating a strong correlation between the two. However, it is worth noting that in ENF sites, there is a trend of increasing NPP with increasing VPD in the 30–50% SWC range, and NPP in the 70–100% and 0–15% SWC ranges is very similar and significantly decreases with increasing VPD.

To facilitate a more intuitive comparison of the effects of VPD and SWC on Gs, GPP, and NPP, we analyzed the variability in these three variables at various VPD and SWC percentiles (Figure 4). By dividing Gs, GPP, and NPP into 10 × 10 grids based on every 10th percentile of VPD and SWC, with red indicating positive changes and blue indicating negative changes, we found that the five vegetation types exhibited clear stratification in VPD and SWC. The CRO and DBF sites showed a clear boundary around the 30th percentile of SWC, where Gs, GPP, and NPP exhibited significant negative changes below this value and positive changes above it. The DBF sites were more significantly affected by

VPD, with the required SWC for positive changes increasing with higher VPD. In contrast, the CRO sites were more affected by VPD at extremely high SWC levels (90–100%), with all three indicators gradually increasing with increasing VPD (variability ranging from −10% to +20%), further confirming the conclusions drawn in Figure 3. The GRA and SAV showed similar variability distributions, but unlike the previous two vegetation types, they exhibited a clear boundary at the 60–70% percentile of SWC, with a large span of variability ranging from −40% to +40%. This phenomenon indicates that stomatal behavior and productivity in these two vegetation types are significantly affected by SWC and require higher SWC to maintain high stomatal conductance and productivity. However, these two vegetation types have a higher adaptability to atmospheric drought, as they exhibit only small negative changes in Gs, GPP, and NPP at higher SWC levels (70–100%) and under extremely high VPD conditions (90–100%). The change trend for ENF was the most unique, with the distribution of Gs and GPP for this vegetation type clearly affected by both VPD and SWC. Positive changes were observed when the SWC percentile was greater than 10%, but this change was restricted by VPD and only partially alleviated at higher SWC percentiles (80–100%). However, at moderate SWC percentiles (40–70%), the restriction by VPD was severe, and negative changes occurred only when the VPD percentile was greater than 20%, with Gs and GPP levels even lower than those at lower SWC levels (10–30%). In addition, the abnormal increase in NPP observed at the 30–50% percentile of SWC in Figure 3i is also reflected in Figure 4m.

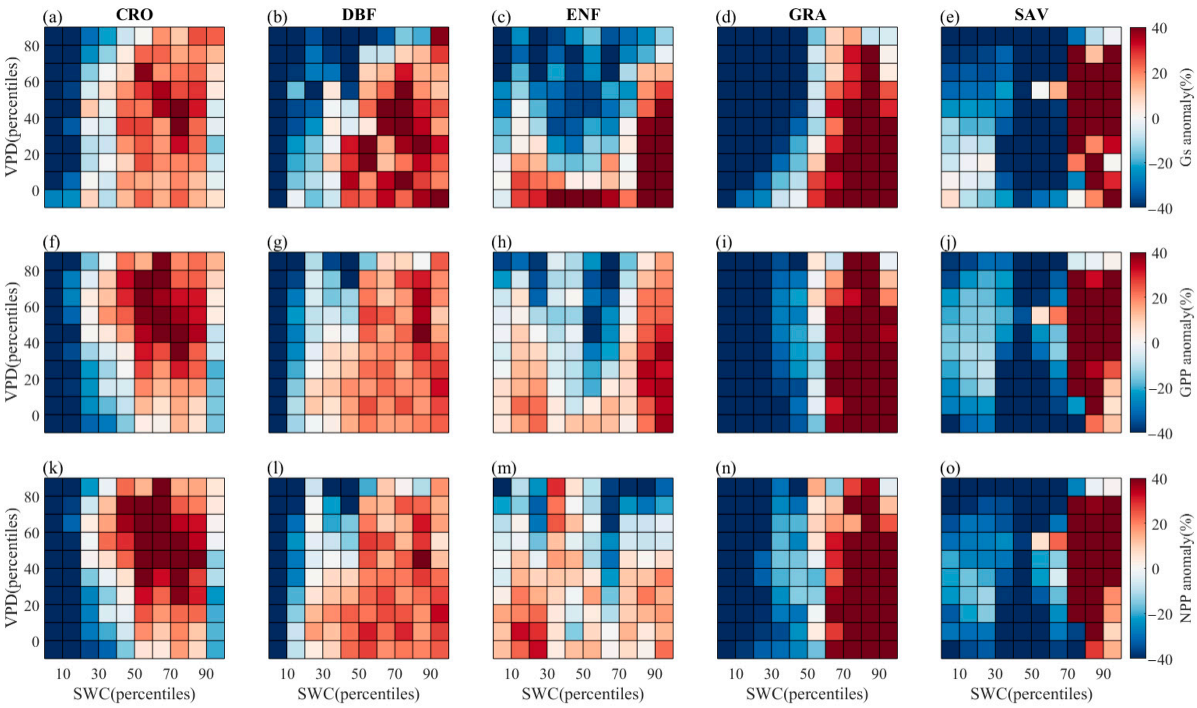

Figure 4. Changes in Gs (**a**–**e**), GPP (**f**–**j**), and NPP (**k**–**o**) affected by VPD and SWC for five PFTs (CRO, DBF, ENF, GRA, SAV). The color in the figure indicates the abnormality of Gs, GPP, CUE, and WUE for each VPD and SWC percentile. For different vegetation types, the difference between these variables and the average value of the multi-year growing season is calculated as the abnormal value on the hourly scale.

3.3. Influence of VPD and SWC on WUE and CUE of Different PFTs

In the previous section, we found that VPD and SWC limit the Gs, GPP, and NPP of vegetation, which directly affect the WUE and CUE of vegetation. To further investigate the effects of VPD and SWC on WUE and CUE, we used a similar analytical approach as in the previous section and focused on the possible impact of VPD and SWC on WUE and CUE. From Figure 5, it is clear that the linear relationship between WUE/CUE and VPD/SWC is not as strong as that between Gs/GPP and VPD/SWC. Overall, in the five vegetation types, WUE generally increases with increasing VPD, except for when the soil water content is extremely high (90–100%) in the DBF sites and when the soil water content is between 15 and 30% in the GRA sites under the condition that VPD is greater than 3 kPa, where WUE shows a significant decreasing trend. The effect of SWC is more ambiguous, as WUE in the DBF and ENF sites with lower soil water content (15–30%) is higher in than those with higher soil water content (90–100%). These conclusions are also supported by Figure 6, which shows that positive changes in WUE are mainly distributed in the upper part of the 10 × 10 grid, while negative changes are distributed in the lower part. The area with the greatest positive change in WUE among the five vegetation types is mainly located in the 0–50% soil water content percentile and VPD greater than the 40th percentile interval (positive variation of 20–30%), and it is noteworthy that GRA also shows an abnormal positive change in WUE in the 80–90% soil water content percentile interval. As GPP and NPP have a similar distribution with respect to SWC and VPD among the five vegetation types, the specific changes in CUE are difficult to determine from Figures 5 and 6. However, in the previous section, we found that in ENF, the increase in NPP in the 30–50% soil water content percentile range with increasing VPD and the significant decrease in the soil water content percentile range of 70–100% and 0–15% with increasing VPD indirectly leads to an increase or decrease in CUE in these soil water content percentile ranges with increasing VPD.

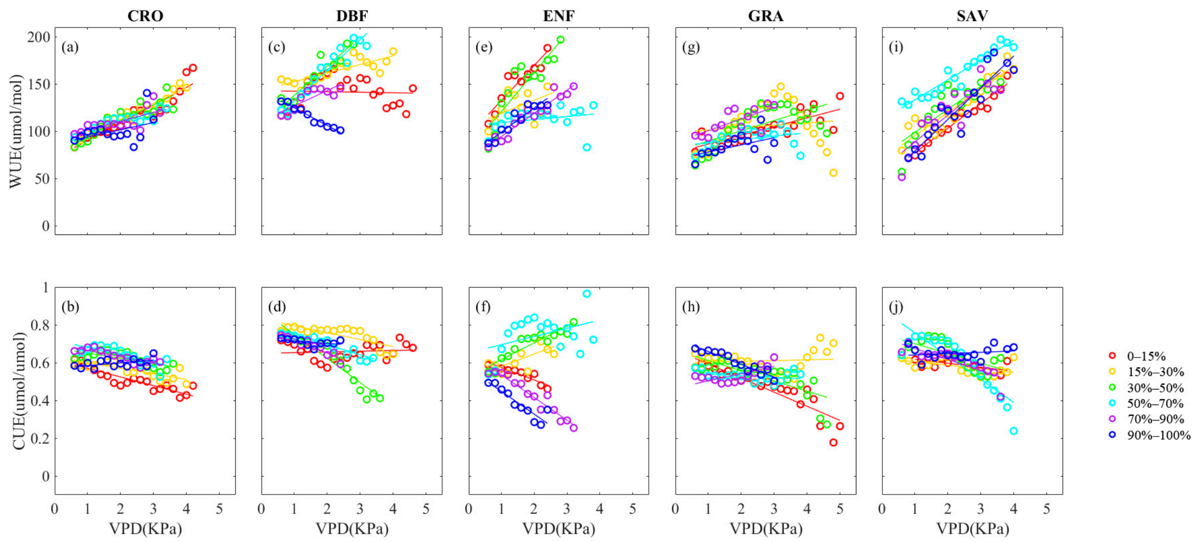

Figure 5. The WUE and CUE of five PFTs (CRO (**a**,**b**), DBF (**c**,**d**), ENF (**e**,**f**), GRA (**g**,**h**), SAV (**i**,**j**)) when VPD and SWC are decoupled. The six colors represent different percentile ranges of soil water content (0–15%, 15–30%, 30–50%, 50–70%, 70–90%, and 90–100%). The interval of each point on VPD is 0.2 kpa.

To further analyze the impact of increased vapor pressure deficit (VPD) and decreased soil water content (SWC) on five different types of vegetation, we quantified the water use efficiency (WUE) and carbon use efficiency (CUE) of different vegetation types under the influence of VPD and SWC, respectively. Figure 7 quantifies the stress of WUE (CUE) under VPD and SWC by subtracting the maximum WUE (CUE) in the highest VPD chamber from the minimum WUE (CUE) in the lowest VPD chamber or by subtracting the minimum WUE (CUE) in the lowest SWC chamber from the maximum WUE (CUE) in the highest SWC chamber (represented as ΔWUE(CUE)(VPD | SWC) and ΔWUE(CUE)(SWC | VPD), respectively).

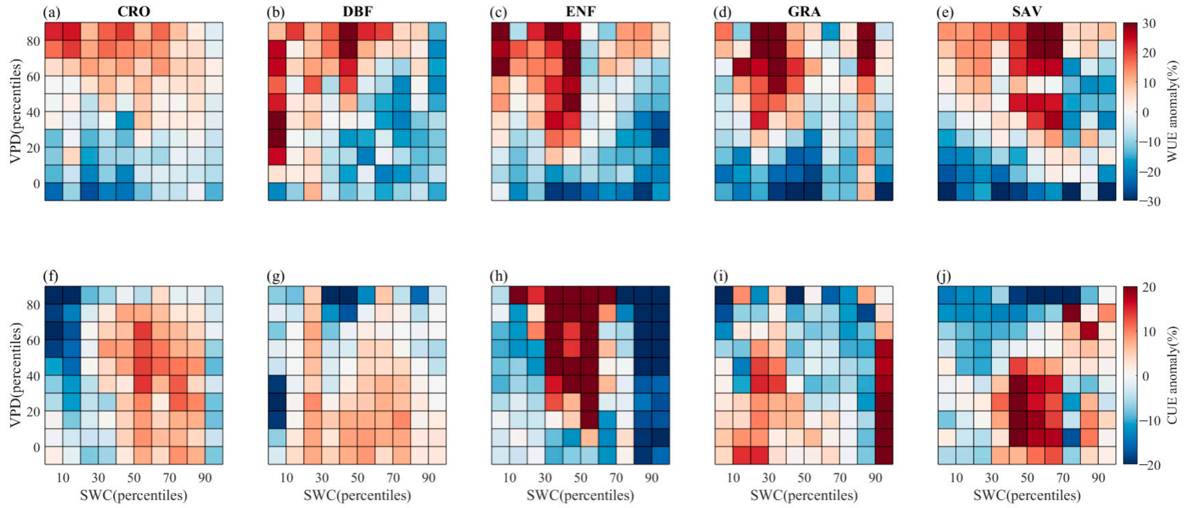

Figure 6. Changes in WUE (**a**–**e**) and CUE (**f**–**j**) affected by VPD and SWC for five PFTs (CRO, DBF, ENF, GRA, SAV).

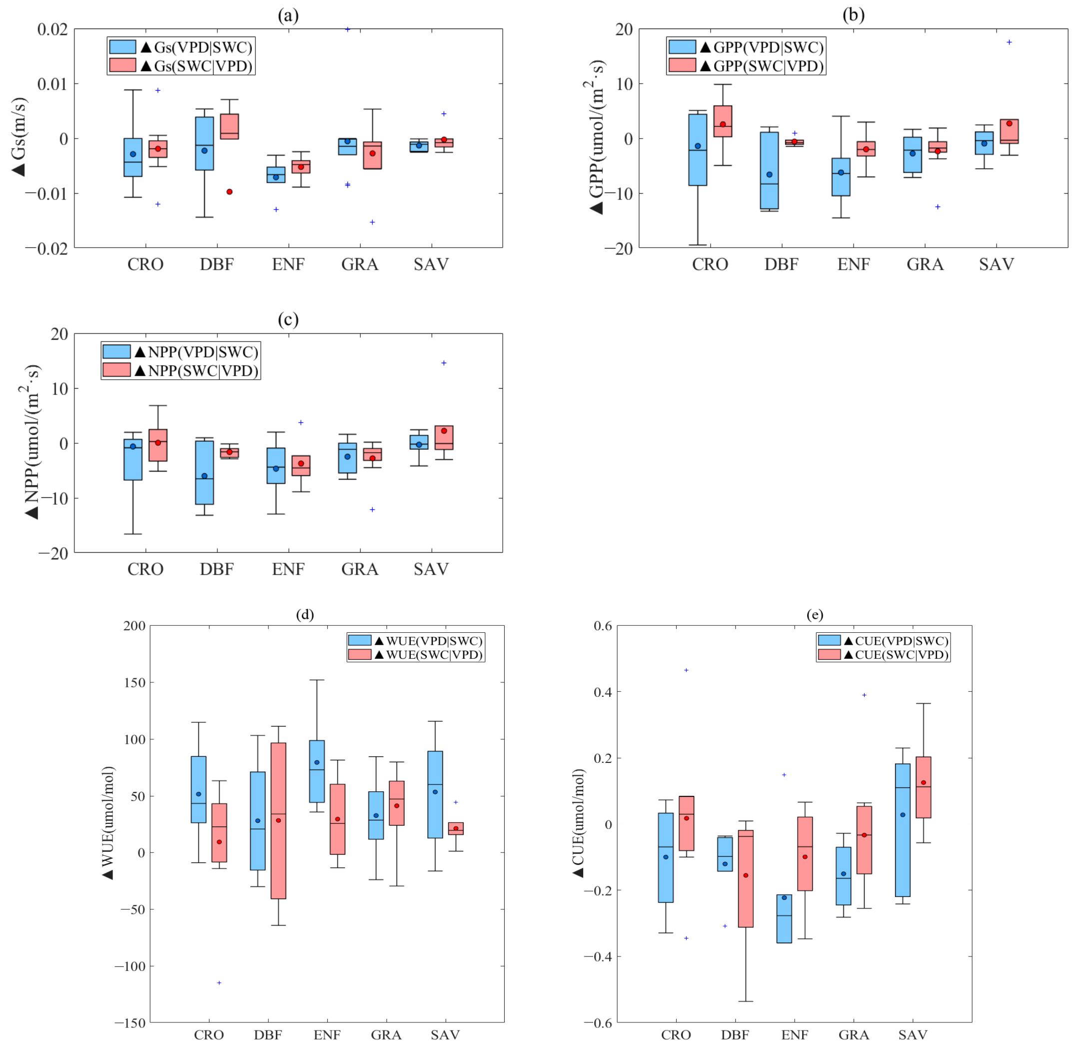

Figure 7. Changes in (**a**) Gs, (**b**) GPP, (**c**) NPP, (**d**) WUE and (**e**) CUE for PFTs (CRO, DBF, ENF, GRA, SAV) under the guidance of increasing VPD (VPD | SWC) and decreasing SWC (SWC | VPD), respectively. The horizontal line represents the median, the point represents the average, and the '+' sign represents the abnormal value.

The results showed that under the influence of VPD and SWC on WUE, an increase in VPD and a decrease in SWC both led to an increase in WUE, with the dominant effect of VPD occurring at around 50 μmol/mol and the ENF vegetation type showing the largest impact at 70 μmol/mol. The change in WUE dominated by a decrease in SWC was around 30 μmol/mol, with a median level consistent across all vegetation types, except for DBF, which showed more significant fluctuations. It should be noted that, in general, high VPD and low SWC limit the GPP and NPP of the plant.

When CUE was studied, an increase in VPD led to a decrease in CUE in CRO, DBF, ENF, and GRA, with the exception of ENF (ΔCUE(VPD | SWC) = −0.28), where the change in CUE for the other three vegetation types was around −0.1 μmol/μmol. In contrast, the change in CUE dominated by a decrease in SWC were much smaller, with the median of ΔCUE(SWC | VPD) fluctuating around −0.05 μmol/μmol for all three vegetation types, except for the CRO and SAV vegetation types, indicating that the influence of SWC is limited compared to VPD. In contrast to the previous four vegetation types, the SAV vegetation type showed an increasing trend in CUE with both an increase in VPD and a decrease in SWC, with the median of both ΔCUE(SWC | VPD) and ΔCUE(VPD | SWC) being 0.1 μmol/μmol, indicating that an increase in VPD and a decrease in SWC have a significant promoting effect on CUE in the SAV vegetation type.

4. Discussion

The results showed the effects of the decoupling of VPD and SWC on the stomatal behavior of the vegetation. It is evident that Gs in the five vegetation types has a significant relationship with VPD and SWC, as Gs decreases significantly with increasing VPD and decreasing SWC. The limitation of the VPD is mostly manifested as a decrease in Gs with increasing VPD across the five vegetation types, indicating that the elevated VPD restricts Gs to varying degrees in different vegetation types, a result that has been confirmed by numerous studies [13,15,40].

VPD dominates the decrease in Gs, GPP, and NPP in most of the vegetation, which has been confirmed in previous studies. In addition, we found that SWC also plays a non-negligible role, which is reflected by the fact that the decrease in SWC limits the overall levels of Gs, GPP, and NPP. While previous studies focused on a single vegetation type (e.g., crop, forest) or separated the effects of VPD and SWC from all types of flux sites as a whole, this paper separates the sites of five representative vegetation types to study their responses to VPD increase and SWC decrease, respectively. Different vegetation types were limited by SWC in a different way, among which CRO and GRA were most limited by SWC, and it is also noted that there is an exceptional response of SAV to SWC, which showed that Gs at low SWC was greater than Gs at high SWC. With respect to VPD, VPD stress is more pronounced in agricultural and forest areas than in shrub and grassland areas.

CRO and DBF exhibit negative variations in Gs, GPP, and NPP when SWC is below the 30th percentile, while GRA and SAV exhibit stronger adaptability to decreased SWC and only exhibit negative variations when SWC is below the 60th percentile. VPD has a more significant impact on the stomatal behavior of vegetation in CRO, DBF, and ENF, while its impact is smaller in GRA and SAV and mainly concentrated in the extremely high VPD range (90–100%). Similar conclusions have been drawn in previous studies, suggesting that VPD stress is stronger in agricultural and forest areas than in shrub and grassland areas, which is due to VPD limitations being more apparent in humid areas than in dry areas [40,41]. Our study also confirms that an increase in VPD has a dominant effect on the increase in WUE, which is similar to the conclusion drawn by Zhang et al. [18]. However, it is worth noting that for the DBF and GRA vegetation types, the decrease in SWC has a greater effect on WUE than the increase in VPD. In addition, we introduced CUE to quantify the carbon sequestration capacity of plants affected by VPD and SWC, and the results showed that an increase in VPD dominated the decrease in CUE in the CRO, DBF, ENF, and GRA vegetation types.

VPD and SWC could affect vegetation WUE and CUE by influencing plant physiological functions in many ways. Under the condition of high VPD and low SWC, plants may be limited in their ability to perform photosynthesis, the process through which plants convert carbon dioxide and water into organic matter using sunlight, producing nutrients and energy for plant growth and metabolism. When water is scarce, plants may close their stomata to reduce water transpiration, thereby reducing the rate of carbon dioxide entry into the leaves, leading to limited photosynthesis and lower water use efficiency. Moreover, when soil moisture is inadequate, plant growth rate may decrease, resulting in reduced efficiency of water use for growth. Plants may adjust their physiological metabolism to adapt to water-limited environments under drought conditions. For example, plants may synthesize and accumulate antioxidant substances to counteract oxidative stress caused by drought. However, the synthesis of these substances requires energy and nutrients, which may lower the total primary productivity and net primary productivity of plants, thereby affecting WUE and CUE.

Less water supply from the soil to the root system induces the plant to reduce water loss and increase WUE through circulating abscisic acid (ABA) with reduced stomatal conductance [42]. Abscisic acid is a plant hormone that plays a crucial role in regulating various physiological processes, especially in response to environmental stress, such as water stress, cold, and drought. When plants experience water stress, ABA is synthesized in certain plant tissues and then transported to other plant organs, where it acts as a signaling molecule to trigger various adaptive responses, such as stomatal closure, regulating gene expression and metabolic processes, or regulating root growth, etc. [43–45]. Together, this generates a limitation through a decrease in the photosynthetic efficiency, GPP, and NPP of the plant.

These adjustments and responses of physiological functions may result in decreased photosynthetic efficiency, total primary productivity, and net primary productivity of vegetation, thereby affecting water use efficiency of vegetation. As is shown in this study, it should be noted that different plant species may exhibit different physiological responses to water stress, thus WUE and CUE may be influenced differently by high vapor pressure deficit and low soil moisture content for different plant species.

5. Conclusions

This research analyzed hourly meteorological flux data from 36 flux sites across five vegetation types worldwide (CRO, DBF, ENF, GRA, SAV) to investigate how variables such as VPD and SWC affect vegetation stomatal behavior and productivity for different types of vegetation. It was found that these variables have a significant impact on ecosystem WUE and CUE, indicating the importance of understanding how they affect ecosystems. The following conclusions were drawn:

(1) High VPD coupled with low SWC can restrict plant stomatal conductance, GPP, and NPP. However, in some vegetation types (CRO, DBF), high soil moisture content can offset the negative impact of high VPD, while low SWC limits vegetation stomatal conductance. Interestingly, in SAV, lower SWC levels (percentiles 0–30%) can lead to higher stomatal conductance and GPP than higher SWC levels (percentiles 30–70%). For certain PFTs, higher soil moisture levels can alleviate the limitation caused by high VPD and even partially promote GPP and NPP as VPD increases. Notably, there is an anomalous increase in NPP in the ENF vegetation type when soil moisture percentiles range between 30 and 50%, leading to a corresponding increase in CUE as soil moisture content increases with VPD.

(2) Vegetation stomatal conductance and productivity have a direct impact on both WUE and CUE. Across the various vegetation types, an increase in VPD generally results in an increase in WUE, while the influence of SWC on WUE is less clear. Moreover, specific analyses reveal that the effect of VPD on WUE is more significant than that of SWC. The changes in WUE due to increasing VPD occur at an average WUE value of approximately 50 μmol/mol, with the ENF vegetation type being the most affected at

70 μmol/mol. Conversely, the changes in WUE due to decreasing SWC occur at an average WUE value of about 30μmol/mol.

(3) The CUE of the CRO, DBF, ENF, and GRA vegetation types decreases as VPD increases, whereas the impact of SWC on these four types is relatively insignificant, with only a −0.05 μmol/μmol total change. In contrast, the SAV vegetation type's CUE is affected differently by VPD and SWC, displaying an ascending tendency in CUE changes that are dominated by the rise in VPD and decline in SWC. This indicates that a decrease in SWC and increase in VPD foster the enhancement of CUE in the SAV vegetation type to some extent.

Supplementary Materials: The following supporting information can be downloaded at: https://www.mdpi.com/article/10.3390/w15091675/s1, Table S1: Station ID, latitude (°), longitude (°) and plant functional type of the 36 Selected flux stations.

Author Contributions: Conceptualization, Y.T. and Z.X.; methodology, Xinran Xia; writing—original draft preparation, Y.T., X.X. and Z.X.; writing—review and editing, Z.L. All authors have read and agreed to the published version of the manuscript.

Funding: This research was funded by the Regional Innovation Development Joint Project of National Natural Science Foundation of China (U21A2021), National Natural Science Foundation of China (U2040212), and China Three Gorges Corporation Research Project (Contract No: 202103429, 202203050).

Data Availability Statement: The fluxnet data are available in the following website: http://fluxnet.fluxdata.org/data/Fluxnet2015dataset/, accessed on 16 June 2020.

Acknowledgments: The authors would like to express their appreciation to the fluxnet website for sharing the observing flux dataset for the research and to the editor and the anonymous reviewers, who provided very helpful comments to improve the manuscript.

Conflicts of Interest: The authors declare no conflict of interest.

References

1. Liu, L.; Gudmundsson, L.; Hauser, M.; Qin, D.; Li, S.; Seneviratne, S.I. Soil moisture dominates dryness stress on ecosystem production globally. *Nat. Commun.* **2020**, *11*, 1723–2041. [CrossRef] [PubMed]
2. Madadgar, S.; AghaKouchak, A.; Farahmand, A.; Davis, S.J. Probabilistic estimates of drought impacts on agricultural production. *Geophys. Res. Lett.* **2017**, *44*, 7799–7807. [CrossRef]
3. Sadras, V.O.; Milroy, S.P. Soil-water thresholds for the responses of leaf expansion and gas exchange: A review. *Field Crops Res.* **1996**, *47*, 253–266. [CrossRef]
4. Huang, C.-W.; Domec, J.-C.; Ward, E.J.; Duman, T.; Manoli, G.; Parolari, A.J.; Katul, G.G. The effect of plant water storage on water fluxes within the coupled soil-plant system. *New Phytol.* **2016**, *213*, 1093–1106. [CrossRef] [PubMed]
5. Martínez-Vilalta, J.; Poyatos, R.; Aguadé, D.; Retana, J.; Mencuccini, M. A new look at water transport regulation in plants. *New Phytol.* **2014**, *204*, 105–115. [CrossRef]
6. Grossiord, C.; Buckley, T.N.; Cernusak, L.A.; Novick, K.A.; Poulter, B.; Siegwolf, R.T.W.; Sperry, J.S.; McDowell, N.G. Plant responses to rising vapor pressure deficit. *New Phytol.* **2020**, *226*, 1550–1566. [CrossRef]
7. Monteith, J.L. A reinterpretation of stomatal responses to humidity. *Plant Cell Environ.* **1995**, *18*, 357–364. [CrossRef]
8. Zhou, S.; Williams, A.P.; Berg, A.M.; Cook, B.I.; Zhang, Y.; Hagemann, S.; Lorenz, R.; Seneviratne, S.I.; Gentine, P. Land–atmosphere feedbacks exacerbate concurrent soil drought and atmospheric aridity. *Proc. Natl. Acad. Sci. USA* **2019**, *116*, 18848–18853. [CrossRef]
9. Zhou, S.; Zhang, Y.; Park Williams, A.; Gentine, P. Projected increases in intensity, frequency, and terrestrial carbon costs of compound drought and aridity events. *Sci. Adv.* **2019**, *5*, eaau5740. [CrossRef]
10. Yuan, F.; Liu, J.; Zuo, Y.; Guo, Z.; Xu, X. Rising vegetation activity dominates growing water use efficiency in the asian permafrost region from 1900 to 2100. *Sci. Total Environ.* **2020**, *736*, 139587. [CrossRef]
11. Zanotelli, D.; Montagnani, L.; Manca, G.; Tagliavini, M. Net primary productivity, allocation pattern and carbon use efficiency in an apple orchard assessed by integrating eddy-covariance, biometric and continuous soil chamber measurements. *Biogeosci. Discuss* **2013**, *10*, 3089–3108. [CrossRef]
12. Zhao, Y.Y.; Amy, L.M.; Miao, F.F.; Chen, G.; Zhu, X.G. The evolution of stomatal traits along the trajectory toward c4 photosynthesis. *Plant Physiol.* **2022**, *190*, 441–458. [CrossRef] [PubMed]

13. Novick, K.A.; Ficklin, D.L.; Stoy, P.C.; Williams, C.A.; Bohrer, G.; Oishi, A.C.; Papuga, S.A.; Blanken, P.D.; Noormets, A.; Sulman, B.N.; et al. The increasing importance of atmospheric demand for ecosystem water and carbon fluxes. *Nat. Clim. Chang.* **2016**, *6*, 1023–1027. [CrossRef]
14. Sulman, B.N.; Roman, D.T.; Yi, K.; Wang, L.; Phillips, R.P.; Novick, K.A. High atmospheric demand for water can limit forest carbon uptake and transpiration as severely as dry soil. *Geophys. Res. Lett.* **2016**, *43*, 9686–9695. [CrossRef]
15. Kimm, H.; Guan, K.; Gentine, P.; Wu, J.; Bernacchi, C.J.; Sulman, B.N.; Griffis, T.J.; Lin, C. Redefining droughts for the U.S. Corn Belt: The dominant role of atmospheric vapor pressure deficit over soil moisture in regulating stomatal behavior of Maize and Soybean. *Agric. For. Meteorol.* **2020**, *287*, 107930. [CrossRef]
16. Franks, P.J.; Adams, M.A.; Amthor, J.S.; Barbour, M.M.; Berry, J.A.; Ellsworth, D.S.; Farquhar, G.D.; Ghannoum, O.; Lloyd, J.; McDowell, N.; et al. Sensitivity of plants to changing atmospheric CO2concentration: From the geological past to the next century. *New Phytol.* **2013**, *197*, 1077–1094. [CrossRef]
17. Nie, C.; Huang, Y.; Zhang, S.; Yang, Y.; Zhou, S.; Lin, C.; Wang, G. Effects of soil water content on forest ecosystem water use efficiency through changes in transpiration/evapotranspiration ratio. *Agric. For. Meteorol.* **2021**, *308–309*, 108605. [CrossRef]
18. Zhang, Q.; Ficklin, D.L.; Manzoni, S.; Wang, L.; Way, D.; Phillips, R.P.; Novick, K.A. Response of ecosystem intrinsic water use efficiency and gross primary productivity to rising vapor pressure deficit. *Environ. Res. Lett.* **2019**, *14*, 074023. [CrossRef]
19. Keenan, T.F.; Hollinger, D.Y.; Bohrer, G.; Dragoni, D.; Munger, J.W.; Schmid, H.P.; Richardson, A.D. Increase in forest water-use efficiency as atmospheric carbon dioxide concentrations rise. *Nature* **2013**, *499*, 324–327. [CrossRef]
20. Knauer, J.; Zaehle, S.; Medlyn, B.E.; Reichstein, M.; Williams, C.A.; Migliavacca, M.; de Kauwe, M.G.; Werner, C.; Keitel, C.; Kolari, P.; et al. Towards physiologically meaningful water-use efficiency estimates from eddy covariance data. *Glob. Chang. Biol.* **2017**, *24*, 694–710. [CrossRef]
21. Mastrotheodoros, T.; Pappas, C.; Molnar, P.; Burlando, P.; Keenan, T.F.; Gentine, P.; Gough, C.M.; Fatichi, S. Linking plant functional trait plasticity and the large increase in forest water use efficiency. *J. Geophys. Res. Biogeosci.* **2017**, *122*, 2393–2408. [CrossRef]
22. Zhu, W.Z. Advances in the carbon use efficiency of forest. *Chin. J. Ecol.* **2014**, *37*, 1043–1058. [CrossRef]
23. Stratton, L.C.; Goldstein, G. Carbon uptake, growth and resource-use efficiency in one invasive and six native hawaiian dry forest tree species. *Tree Physiol.* **2001**, *21*, 1327–1334. [CrossRef] [PubMed]
24. Dong, G.; Guo, J.; Chen, J.; Ge, S.; Song, G.; Hu, L.; Wang, Y. Effects of spring drought on carbon sequestration, evapotranspiration and water use efficiency in the songnen meadow steppe in northeast China. *Ecohydrology* **2011**, *4*, 211–224. [CrossRef]
25. Linares, J.C.; Delgado-Huertas, A.; Camarero, J.J.; Carreira, M. Competition and drought limit the response of water-use efficiency to rising atmospheric carbon dioxide in the mediterranean fir abies pinsapo. *Oecologia* **2009**, *161*, 611–624. [CrossRef]
26. Zouaoui, R.; Ksontini, M.; Ourry, A.; Ferchichi, A. Effect of drought on leaf gas exchange, water-use efficiency and carbon isotope discrimination in two species (*Rhus tripartitum* (ucria) grande and *Ziziphus lotus* (L.)) in arid zone of tunisia threatened of disappearance. *Int. J. Plant Prod.* **2013**, *4*, 1616–1627.
27. Reichstein, M.; Falge, E.; Baldocchi, D.; Papale, D.; Aubinet, M.; Berbigier, P.; Bernhofer, C.; Buchmann, N.; Gilmanov, T.; Granier, A.; et al. Climate extremes and the carbon cycle. *Nature* **2013**, *500*, 287–295. [CrossRef]
28. Lin, C.; Gentine, P.; Huang, Y.; Guan, K.; Kimm, H.; Zhou, S. Diel ecosystem conductance response to vapor pressure deficit is suboptimal and independent of soil moisture. *Agric. For. Meteorol.* **2018**, *250*, 24–34. [CrossRef]
29. Lyons, D.S.; Dobrowski, S.Z.; Holden, Z.A.; Maneta, M.P.; Sala, A. Soil moisture variation drives canopy water content dynamics across the western US. *Remote Sens. Environ.* **2021**, *253*, 112233. [CrossRef]
30. Gentine, P.; Chhang, A.; Rigden, A.; Salvucci, G. Evaporation estimates using weather station data and boundary layer theory. *Geophys. Res. Lett.* **2016**, *43*, 11661–11670. [CrossRef]
31. Green, J.K.; Konings, A.G.; Alemohammad, S.H.; Berry, J.; Entekhabi, D.; Kolassa, J.; Lee, J.-E.; Gentine, P. Regionally strong feedbacks between the atmosphere and terrestrial biosphere. *Nat. Geosci.* **2017**, *10*, 410–414. [CrossRef] [PubMed]
32. Schwalm, C.R.; Williams, C.A.; Schaefer, K.; Baldocchi, D.; Black, T.A.; Goldstein, A.H.; Law, B.E.; Oechel, W.C.; Paw, U.K.T.; Scott, R.L. Reduction in carbon uptake during turn of the century drought in western North America. *Nat. Geosci.* **2012**, *5*, 551–556. [CrossRef]
33. Anderegg, W.R.; Konings, A.G.; Trugman, A.T.; Yu, K.; Bowling, D.R.; Gabbitas, R.; Karp, D.S.; Pacala, S.; Sperry, J.S.; Sulman, B.N.; et al. Hydraulic diversity of forests regulates ecosystem resilience during drought. *Nature* **2018**, *561*, 538–541. [CrossRef] [PubMed]
34. Pastorello, G.; Trotta, C.; Canfora, E.; Chu, H.; Christianson, D.; Cheah, Y.-W.; Poindexter, C.; Chen, J.; Elbashandy, A.; Humphrey, M.; et al. The FLUXNET2015 dataset and the ONEFlux processing pipeline for eddy covariance data. *Nat. Publ. Group* **2020**, *7*, 225. [CrossRef]
35. Monteith, J. Evaporation and surface temperature. *Q. J. R. Meteorol. Soc.* **2007**, *107*, 1–27. [CrossRef]
36. Pennypacker, S.; Baldocchi, D. Seeing the fields and forests: Application of surface-layer theory and flux-tower data to calculating vegetation canopy height. *Bound.-Layer. Meteorol.* **2016**, *158*, 165–182. [CrossRef]
37. Reichstein, M.; Falge, E.; Baldocchi, D.; Papale, D.; Aubinet, M.; Berbigier, P.; Bernhofer, C.; Buchmann, N.; Gilmanov, T.; Granier, A.; et al. On the Separation of Net Ecosystem Exchange into Assimilation and Ecosystem Respiration: Review and Improved Algorithm. *Glob. Chang. Biol.* **2005**, *11*, 1424–1439. [CrossRef]

38. Chambers, J.Q.; Tribuzy, E.S.; Toledo, L.C.; Crispim, B.F.; Higuchi, N.; dos Santos, J.; Araújo, A.C.; Kruijt, B.; Nobre, A.D.; Trumbore, S.E. Respiration from a tropical forest ecosystem: Partitioning of sources and low carbon use efficiency. *Ecol. Appl.* **2004**, *14*, 72–88. [CrossRef]
39. Green, J.K.; Seneviratne, S.I.; Berg, A.M.; Findell, K.L.; Hagemann, S.; Lawrence, D.M.; Gentine, P. Large influence of soil moisture on long-term terrestrial carbon uptake. *Nature* **2019**, *565*, 476–479. [CrossRef]
40. Fu, Z.; Ciais, P.; Prentice, I.C.; Findell, K.L.; Hagemann, S.; Lawrence, D.M.; Gentine, P. Atmospheric dryness reduces photosynthesis along a large range of soil water deficits. *Nat. Commun.* **2022**, *13*, 989. [CrossRef]
41. Wang, H.; Yan, S.; Ciais, P.; Wigneron, J.; Liu, L.; Li, Y.; Fu, Z.; Ma, H.; Liang, Z.; Wei, F.; et al. Exploring complex water stress–gross primary production relationships: Impact of climatic drivers, main effects, and interactive effects. *Glob. Chang. Biol.* **2022**, *28*, 4110–4123. [CrossRef] [PubMed]
42. Qiu, M.; Hao, Z. Sensitivity to abscisic acid regulates stomatal oscillation and closure in arabidopsis thaliana. *Pak. J. Bot.* **2010**, *42*, 353–359.
43. Kucera, B.; Cohn, M.A.; Leubner-Metzger, G. Plant hormone interactions during seed dormancy release and germination. *Seed Sci. Res.* **2005**, *15*, 281–307. [CrossRef]
44. Leung, J.; Giraudat, J. Abscisic acid signal transduction. *Ann. Rev. Plant Biol.* **1998**, *49*, 199. [CrossRef]
45. Yue, M.; Szostkiewicz, I.; Korte, A.; Moes, D.; Yang, Y.; Christmann, A.; Grill, E. Regulators of pp2c phosphatase activity function as abscisic acid sensors. *Science* **2009**, *324*, 1064–1068.